Nuclear Inst. and Methods in Physics Research, A 975 (2020) 164200

Contents lists available at ScienceDirect

Nuclear Inst. and Methods in Physics Research, A

journal homepage: www.elsevier.com/locate/nima

A general-purpose digital data acquisition system (GDDAQ) at Peking University

H.Y. Wu [a], Z.H. Li [a,*], H. Tan [b], H. Hua [a,*], J. Li [a], W. Hennig [b], W.K. Warburton [b], D.W. Luo [a], X. Wang [a], X.Q. Li [a], S.Q. Zhang [a], C. Xu [a], Z.Q. Chen [a], C.G. Wu [a], Y. Jin [a], J. Lin [a], D.X. Jiang [a], Y.L. Ye [a]

[a] State Key Laboratory of Nuclear Physics and Technology, School of Physics, Peking University, Beijing 100871, China
[b] XIA LLC, 31057 Genstar Rd., Hayward, CA 94544, USA

ARTICLE INFO

Keywords:
Digital data acquisition system
Trigger
Parameters optimization

ABSTRACT

A general-purpose digital data acquisition system (GDDAQ) has been developed at Peking University. This GDDAQ, composed of 16-channel Digital Pulse Processor Pixie-16 modules from XIA LLC, is a versatile, flexible, and easily expandable data acquisition system for nuclear physics research in China. The software used by this GDDAQ is based on the CERN ROOT framework and developed and tested in CentOS 7 LINUX operating platform. A flexible trigger system has also been developed to accommodate different experimental settings. A user-friendly software GUI helps users monitor and debug the detection system in real timer or offline. Many offline analysis tools have been developed to help users quickly optimize parameters for various types of detectors without the need for time-consuming tests and measurements. This GDDAQ has been successfully implemented in several nuclear physics experiments and its versatility and high efficiency have been demonstrated.

1. Introduction

With their much higher pulse processing flexibilities and easier communication with computer control systems, Digital Data Acquisition Systems (DDAQs) have been used extensively in recent years and have demonstrated significant advantages over conventional analog systems in nuclear physics research [1–5], like studies of short-lived charged particle emitters which involve overlapping ion–particle or particle–particle signals [6–9] and studies of sub-microsecond isomers observed in fragmentation reactions [10]. With sufficient accuracy to recover the original information of the detector pulses and offering precise control of many experimental parameters, DDAQs have been successfully implemented for nuclear spectroscopy in a wide variety of detector systems: HPGe arrays [11–16], neutron detection arrays [17–19], charge-particle silicon detection arrays [20–22] etc. In general, nuclear spectroscopic information is derived from coincidence measurements between various types of detectors. Consequently, there have been continuous efforts to apply DDAQs to experiments that utilize a large mix of detectors [23–25].

For a general-purpose digital data acquisition system (GDDAQ), the following capabilities are important and necessary:

- Extensible framework. The system should support large numbers of channels and be easily expanded;
- Flexible triggering mode. The trigger setup is flexible enough to accommodate not only large detector arrays but also any ancillary detectors;
- User-friendly parameters adjustment. The system should be remotely controllable and can assist users to quickly optimize experimental parameters;
- Efficient online-monitoring.

The present paper reports a GDDAQ that has been developed at Peking University. Possessing the capabilities mentioned above, this GDDAQ has been successfully implemented in γ-spectroscopy experiments at both the China Institute of Atomic Energy (CIAE) and iThemba LABS in South Africa, at the Back-n Beamline of China Spallation Neutron Source (CSNS) and the β-decay experiments at the Institute of Modern Physics (IMP) in China. This GDDAQ is easy to use without requiring special technical expertise. The present paper is organized as follows: Section 2 presents the DAQ system, Section 3 describes the triggering system. The graphical user interface is presented in Section 4. Lastly, offline optimization is described in Section 5 and a summary is given in Section 6.

* Corresponding authors.
E-mail addresses: zhli@pku.edu.cn (Z.H. Li), hhua@pku.edu.cn (H. Hua).

https://doi.org/10.1016/j.nima.2020.164200
Received 20 March 2020; Received in revised form 20 May 2020; Accepted 28 May 2020
Available online 30 May 2020
0168-9002/

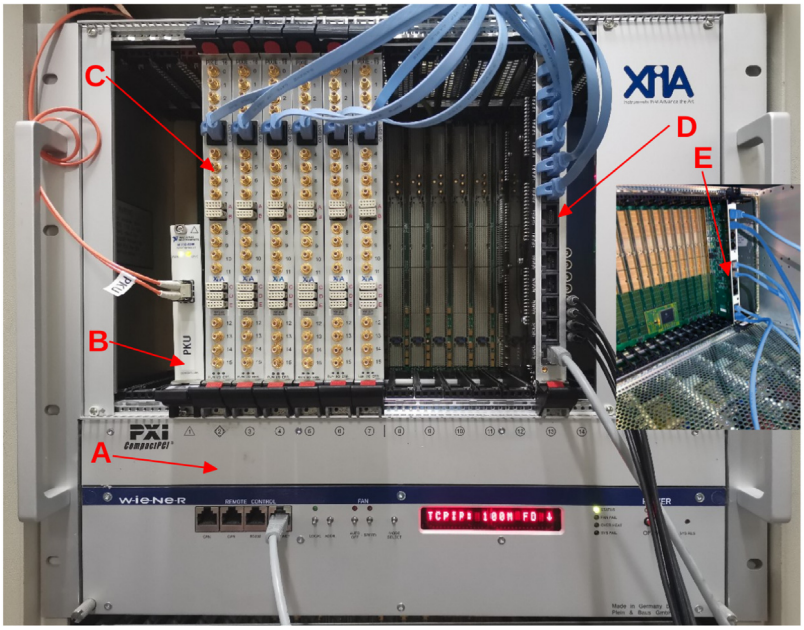

Fig. 1. GDDAQ small scale 96-channel system unit. The blue network cables are used to transmit logic signals, and the gray network cables are used to connect to the network for remote monitoring of the chassis. (For interpretation of the references to color in this figure legend, the reader is referred to the web version of this article.)

2. Description of DAQ system

2.1. Hardware

The principal components of the hardware for this GDDAQ are Pixie-16 modules and support cards manufactured by XIA LLC [26] and others: (See arrows in Fig. 1)

(A) Pixie-16 6U CompactPCI/PXI chassis
(B) PCI-8366/PXI-8368, chassis controller [27]
(C) Pixie-16, 12/14/16 bits, 100/250/500 MSPS ADC
(D) Pixie-16 MicroZed-based Trigger I/O (MZTIO), a programmable trigger module
(E) Pixie-16 clock and trigger rear I/O module

Fig. 1 shows a typical example of this GDDAQ. The Pixie-16 modules reside in slots in the Pixie-16 chassis, which is based on CompactPCI/PXI standards, allowing experimental data transfer from module memories to the host computer at a rate up to 109 MByte/s. The system communication and control occur through the PCI-8366/PXI-8368 module via fiber optic cable. For an extensible GDDAQ, synchronization of clock and distribution of triggers between separate chassis is necessary. This functionality is provided by the Pixie-16 clock and trigger rear I/O module [5], which can currently synchronize up to a maximum of 8 chassis (1600 channels). The MZTIO [28] is designed to route signals between the PXI backplane and the chassis front panel and make logical combinations between them in field programmable gate array (FPGA) fabric. It also supports the IEEE 1588 precision time protocol (PTP) and can synchronize the chassis clock to a PTP master clock.

2.2. Firmware and software framework

In GDDAQ, the experimental information stored in each channel is user controllable. Users can determine whether to record raw baseline, charge integral, external timestamps and/or waveforms. In standard Pixie-16 firmware, once the waveform buffer is full in the waveform recoding mode, no subsequent events can be stored until the buffer is cleared. This will result in loss of real events in the presence of high counting rates. Thus, to increase flexibility of the system, special Pixie-16 firmware was developed specifically for the GDDAQ such that while the waveform buffer is full at high counting rate, only key information of the event will be stored, e.g. time-stamp and amplitude, but not the whole waveform.

Fig. 2 shows a typical configuration of this GDDAQ. All the components of the GDDAQ communicate with each other via the network. Software based on the CERN ROOT framework [29] has been developed on LINUX and tested under the CentOS 7 platform. The following software has been developed to conveniently handle the experimental data: Controller (acquisition control), Online and Decoder.

The operation of a multi-unit GDDAQ is as follows. Output signals from detector preamplifiers/PMTs are first digitized by the Pixie-16 and further signal processing is then performed by a set of real-time signal processing algorithms in the firmware [30]. Once a physics event is identified by either local or external trigger logic, the event data are recorded first in the FPGA local memory and then stored in the external First-In First-Out (FIFO) memory. The data in the FIFO are transferred to the host computer via the fiber optical cable, and finally to the data storage center via Ethernet. Each module has its own data file and recorded data from its channels are stored in binary format for further offline analysis. Raw data are converted to a ROOT-data format file by a decoding program (Decoder, Fig. 2), and an event-building program reconstructs absolute timing information for each event from different modules and re-organizes the data to an event-by-event structure. Some basic sample code which users can use to develop their own analysis programs has also been included in the software package.

Periodically (every 3 s in the present GDDAQ), real-time run data stored in the Pixie-16 modules' memories (e.g. the data throughput rate, trigger rate, and each channel's energy, etc.), can be monitored by online processes through a shared memory mechanism (Online, Fig. 2). Consequently, the DAQ's efficiency is improved greatly without the need to decode data in real time to provide basic online monitoring functions. In addition, the software's main control interface (Controller, Fig. 2) serves as the hub for acquisition control, parameters adjustment and offline parameters optimization, etc.

3. Trigger

The recent introduction of triggerless DDAQs, which record all live events without event selection, has provided an attractive option for users [31]. However, while they bring great flexibility for offline data

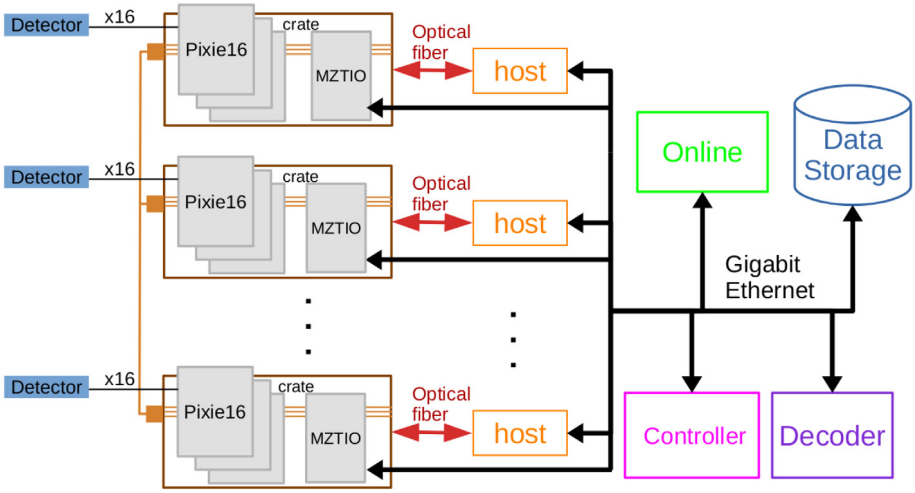

Fig. 2. (Color online) GDDAQ archite.

analysis, they can also generate significant data streams in the experiments involving high counting rates, which may then be beyond the DDAQs' I/O capabilities. Therefore, a proper triggering system, which is flexible enough to accommodate different experimental circumstances, is essential for a well designed GDDAQ. The trigger system of the present GDDAQ consists of two interdependent parts: internal trigger and external trigger.

3.1. Internal trigger

When output signals from the preamplifier/PMT cross a threshold preset in a Pixie-16 module, a fast trigger pulse is generated in the Signal Processing FPGA and sent to the System FPGA. Whether the corresponding event is recorded or not also depends on the user-selectable "control logic" which includes module/channel validation triggers, vetoes etc. [24,30]. For standard Pixie-16 firmware, each Pixie-16 module can perform multiplicity and/or coincidence test using both its own input channels and/or its immediate neighbors in system FPGA. Thus, local multiplicity or coincidence among up to 48 channels can be obtained. Further, multiplicity testing with more channels can be realized using custom designed firmware. However the implementation of such custom firmware will be limited by the FPGA's available resources.

3.2. External trigger

To implement efficient and flexible external trigger patterns, a programmable module MZTIO was developed for the GDDAQ. Fig. 3 shows the module with a mezzanine card MEZZ01. It is based on the commercial MicroZed Zynq processor module [32] and a custom carrier board. The Xilinx Zynq processor combines FPGA fabric (for the trigger logic) and an ARM processor (running Linux) on the same chip. The xillybus lite IP core [33] is used to read and write FPGA registers from Linux. All Zynq firmware and software is released as open source by XIA and customized for the present GDDAQ. The carrier board powers the MicroZed board, facilitates the connections from the Pixie-16 chassis backplane to the Zynq FPGA pins, brings out additional FPGA I/O to the front panel via bidirectional Low-voltage Differential Signaling (LVDS) buffers or to headers for mezzanine cards, and provides an Ethernet PHY for the ARM. Besides Ethernet data I/O, this PHY also provides PTP hardware timestamping, a PTP output clock, and programmable GPIO signals. The PTP output clock is connected to the FPGA fabric, a front panel MMCX connector, and the PXI clock distribution lines on the backplane, which allows the MZTIO trigger logic and the Pixie-16's data acquisition clocks to be synchronized with a PTP clock master (frequency, time and date to tens of nanosecond precision) similar to PTP triggering with Pixie-Net modules [34]. Triggering mechanism (shown in Fig. 4(a)) is implemented as follows: the multiplicity triggers Ma and Mb are generated for each selected channel in immediate neighbors 1–3 Pixie-16 modules (If necessary, Mc and Md can also be added) and sent via the RJ-45 connectors to the LVDS inputs of the MZTIO, where the corresponding trigger signal is generated according to user-customized logic and then sent back as module validation trigger of Pixie-16 modules either through the RJ-45 connector or the chassis backplane.

Using Hardware Description Language (HDL), user-customized external triggers are then achieved by programming the FPGA. Some basic functions that make it easy to incorporate various logics in MZTIO, have been developed. For example, the functional modules "SignalDelay" and "SignalExtend", can delay a logic pulse and adjust its width, respectively.

The mezzanine card MEZZ01 with 8 LEMO connectors is mounted in a FPGA I/O header of the MZTIO. Each connector can be programmed individually as input or output. In input mode, signals from other DAQ or detectors can be sent into the MZTIO module to participate in the trigger generation. In output mode, the time relationship between different trigger signals in MZTIO can be monitored by an oscilloscope. Based on observed time relationships, delay and width of trigger signals can be adjusted. In addition, Pixie-16 module signals (Delayed local fast trigger, Stretched module/channel validation trigger and Stretched Veto trigger) can also be monitored by the MZTIO through the chassis backplane.

Fig. 4(b) shows an example of trigger generation for a 64 × 64 double-sided silicon strip detector (DSSD). The TRIGGER1 and TRIGGER2 signals are generated from coincidence of the front and rear sides with multiplicity greater than zero ($M \geq 1$) and one ($M \geq 2$) respectively, to select multi-fragment events. Here, the 64 channels from one side of silicon strip detector are distributed over 4 Pixie-16 modules, where they are divided into four groups: G1, G2, G3, G4, respectively. Multiplicity triggers M1 ($M \geq 1$) and M2 ($M \geq 2$) from each group are combined logically in the MZTIO. The logic diagram in the dashed box of Fig. 4(b) shows the logical OR and AND operations that are done in the MZTIO, while the rectangular boxes flag "GDG" represents the functional module Gate and Delay Generator.

4. Graphical user interface (GUI)

Monitoring and debugging the detection system at all times is important for the success of an experiment, and a user-friendly GUI can help users achieve that goal. Fig. 5 shows a snapshot of the main window of the GDDAQ's GUI. The data collection program is based on

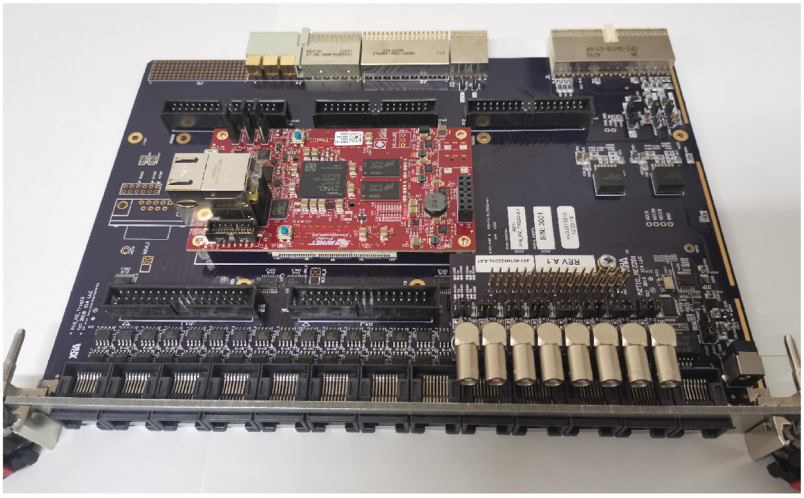

Fig. 3. (Color online) Photograph of a MZTIO with mezzanine card. It is based on a Zynq module [32] with ARM/Linux software for user access to parameters and with FPGA fabric for trigger routing to external electronics.

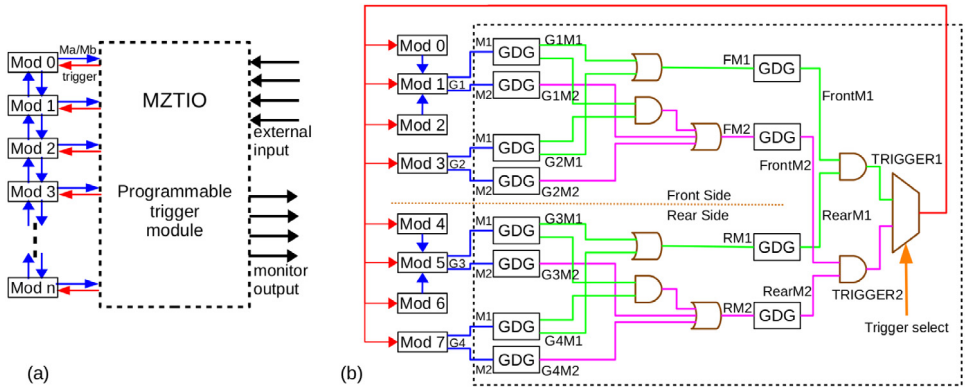

Fig. 4. (Color online) (a) System logic block diagram in the GDDAQ and (b) Example of logic block diagram in 64 × 64 double-sided silicon strip detector.

an earlier version of the NSCL DDAS Nscope program [35]. As shown in Fig. 5, it consists of two parts: control and monitor. To get the useful information and update the experimental parameters efficiently, the present control GUI (Fig. 5(a)) incorporates a top-bar populated with frequently used functions, such as basic parameters setting, logic control, debug and offline parameters optimization analysis, etc. All aspects of the GDDAQ can be easily manipulated from the drop-down of its corresponding control-panel. Fig. 5(b) is one of the pop-up sub-interfaces of Fig. 5(a).

For the control part of the GUI shown in the left side of Fig. 5(a), the "boot" button on the top is used to initialize DAQ. Users can set the file path, file name and run number in the "setup" region. In the "control" region, users can run the start/stop commands. The option box "Online Statistics" is used to decide whether or not to send online monitoring data to Monitor Viewer. The option box "update energy monitor" is used to refresh the online spectrum. The information region shows a simple log of the DAQ system.

The monitor part shown in right side of Fig. 5 has two versions based on different technologies: ROOT GUI and HTML5/CSS/JS. The online ROOT GUI monitor adopted in the present GDDAQ reads experimental information (input trigger rates, output trigger rates, and the energy spectrum etc.) from the shared memory and displays selected messages on the window. The data in shared memory is also stored in the MYSQL database, which the client in the network can access through the web page.

In addition, some web pages have also been developed for MZTIO which can change the acquisition logic of the experiment via setting registers in the FPGA and monitor the trigger rates of the detectors via reading the scaler data from the FPGA.

5. Offline optimization

Precise adjustment of experimental parameters is one of the key requirements for the GDDAQ. For most DDAQs currently in use, optimization of experimental parameters is done in online mode, i.e. with the module on, users adjust the parameters, observe their resulting effects, and repeat until optimized parameters are obtained. For experiments involving a large number of channels, this approach to parameter tuning becomes a time-consuming task. In GDDAQ, we have developed offline tools that can efficiently and quickly optimize parameters for various types of detectors. Waveforms captured by the Pixie-16 modules are analyzed in detail by these offline tools, which call Application Program Interface (API) functions provided by XIA LLC for the analyses. The methods implemented in the APIs are equivalent to the algorithms implemented in the FPGAs. Therefore, the parameters obtained by the offline optimization tools can be directly applied to the modules.

These offline analysis tools used in the present GDDAQ include many different functions, such as filter calculation, threshold optimization, energy parameters optimization, CFD parameters optimization, FFT transformation, etc. These tools make it intuitive for users to easily produce optimized parameters. Here are two examples to illustrate how the tools work.

Threshold optimization: A reasonably low trigger threshold, which can reduce the counting losses of physical events without bringing

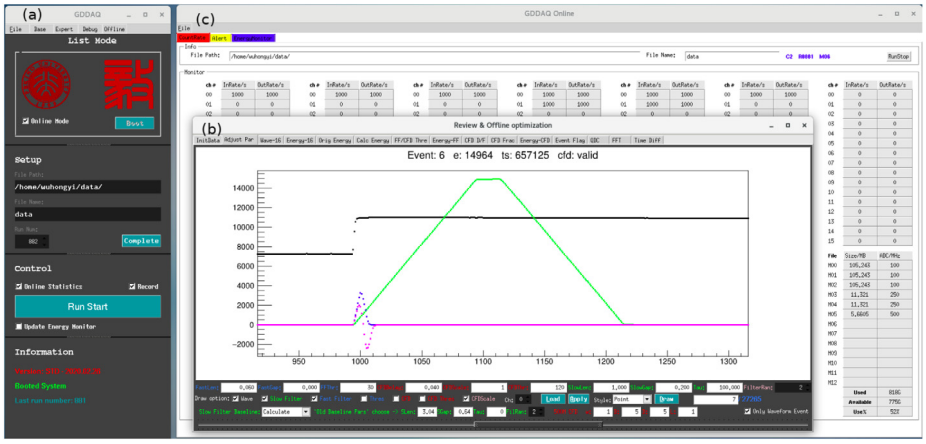

Fig. 5. (Color online) Screenshot of an example GDDAQ User Interface. The left figure (a) shows the main control interface, through which all the acquisition control, parameters adjustment and offline parameters optimization can be completed. The small figure (b) on the right shows the offline parameters optimization interface popped up by the main control interface. The figure (c) on the right shows the online monitoring interface base ROOT GUI, including input/output trigger rate of each channels, file size and other information.

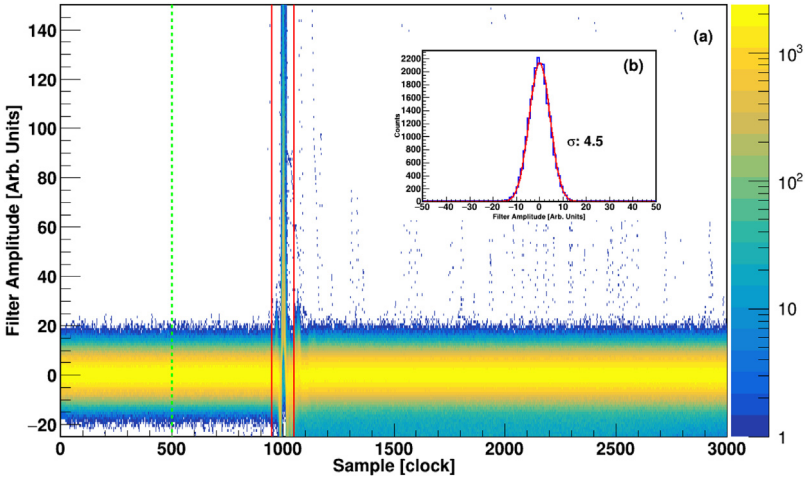

Fig. 6. (Color online) (a) The results of some fast filter response accumulations from silicon detector and the inset (b) shows the y-axis projection of the green dotted line position $x = 500$. (For interpretation of the references to color in this figure legend, the reader is referred to the web version of this article.)

in noise inference, is important for experiments. In GDDAQ, the fast trigger filter response to each original waveform recorded by a channel is calculated individually and accumulated as shown in Fig. 6(a). The area outside the response section of the signal waveform (between the two vertical red lines) is treated as the normal noise region. The lower-limit of the trigger threshold value can then be set as mean value plus 3 to 5 times sigma obtained from a Gaussian fitting to the noise distribution (shown in the inset of Fig. 6(b)), whereas the upper-limit of threshold is determined from the distribution of the maximum value of the noise amplitude within the energy range of interest, which can be obtained from the two-dimensional correlation between amplitudes of pulse and maximum noise (shown in Fig. 7).

CFD parameters optimization: The CFD algorithm [36] detects the zero-crossing of a pulse by subtracting the scaled and delayed copy of the fast filter pulse. The delay and scale parameters should be optimized for each specific application. There are two ways to optimize these two parameters. First, through the distribution of the relative position of the maximum slope in the rising edge of the fast filter waveform, the exact position of the maximum slope can be obtained and used to determine the optimal scale parameter (shown in inset of Fig. 8). Then, by adjusting the delay parameter to have the maximum slope near the zero-crossing point of the CFD filter waveform, the corresponding delay parameters will be selected. The second is to select two channels whose outputs are known to be correlated in time (e.g. detecting the two coincident photons emitted by ^{22}Na), and create their time-difference spectrum. The time resolution of the spectrum can then be calculated with all possible values of delay/scale parameters, allowing users to select the values of delay/scale parameters which result in the best timing resolution.

6. Summary

We reported a general-purpose digital data acquisition system (GDDAQ) developed at Peking University. This GDDAQ is based on Pixie-16 modules from XIA LLC and can be easily expanded to fit acquisition systems of a variety of sizes. Software based on the CERN ROOT framework was developed in LINUX and tested under CentOS 7 platform. A trigger system that is flexible enough to accommodate different experimental circumstances was also developed. A user-friendly GUI helps users to monitor and debug the detection system easily and efficiently. Many offline analysis tools have been developed, which can help users quickly optimize parameters for various types of detectors without long-time test measurements. This GDDAQ has been successfully implemented in several nuclear experiments, and has demonstrated its versatility and high efficiency. It can handle count rates of about 20 k/s for each channel with very little dead time in γ-spectroscopy experiments, and also allows setting relatively low energy thresholds at about 30 keV for the 300-μm-thick DSSD in the β-decay

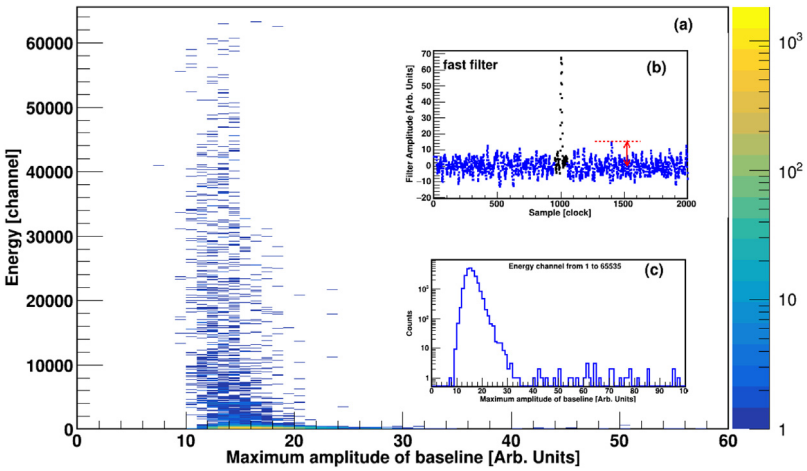

Fig. 7. (Color online) (a) Two-dimensional correlation between energy and maximum value of baseline. The inset (b) shows how to find the maximum value of baseline in a fast filter response, that is, the maximum value in the blue points area. The inset (c) shows baseline projection spectrum of energy channel in the range of 1 to 65535. (For interpretation of the references to color in this figure legend, the reader is referred to the web version of this article.)

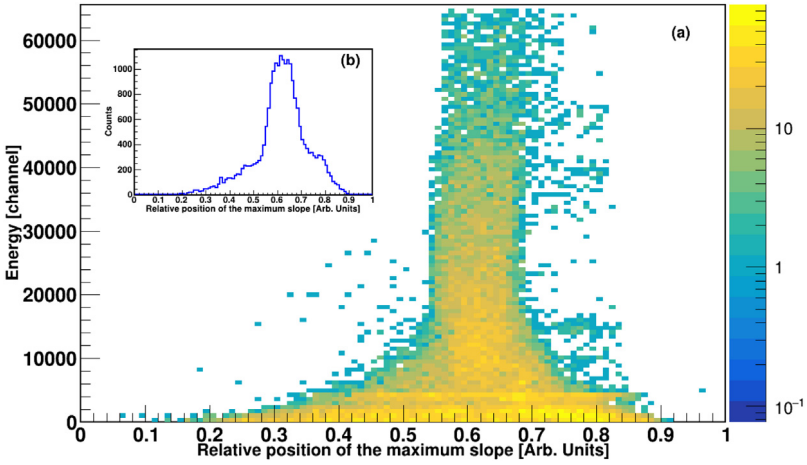

Fig. 8. (Color online) (a) Two-dimensional correlation between amplitudes of pulse and the relative position of the maximum slope in the rising edge of the fast filter waveform. The inset (b) shows (a) projection spectrum of energy channel in the range of 1 to 65535.

experiments. The energy resolution achieved by this GDDAQ is about 0.15% FWHM for the 1408 keV transition of ^{142}Eu with a typical clover detector. In γ-spectroscopy experiments, the energy resolution did not deteriorate when the count rate reached 10 k/s. Some experimental results will be presented in future papers.

All the source code and manual for this work can be found on Github (https://github.com/pkuNucExp/PKUXIADAQ). For instructions on how to use the MZTIO module in this system, please download our instruction manual (https://pkunucexp.github.io/MZTIO/). Next generation software for control and online analysis based on Web-GUI is currently being developed.

CRediT authorship contribution statement

H.Y. Wu: Investigation, Software, Writing - original draft. **Z.H. Li:** Investigation, Resources, Methodology, Funding acquisition. **H. Tan:** Writing - review & editing. **H. Hua:** Writing - review & editing, Funding acquisition. **J. Li:** Software. **W. Hennig:** Writing - review & editing. **W.K. Warburton:** Writing - review & editing. **D.W. Luo:** Software. **X. Wang:** Validation. **X.Q. Li:** Validation. **S.Q. Zhang:** Validation. **C. Xu:** Validation. **Z.Q. Chen:** Validation. **C.G. Wu:** Validation. **Y. Jin:** Validation. **J. Lin:** Validation. **D.X. Jiang:** Validation. **Y.L. Ye:** Validation.

Declaration of competing interest

The authors declare that they have no known competing financial interests or personal relationships that could have appeared to influence the work reported in this paper.

Acknowledgments

This work is supported by the National Key R&D Program of China (Contract No. 2018YFA0404403), the National Natural Science Foundation of China under Grant No. 11775003, No. 11675003, No. 11575006, No. 11875075. We appreciate Z. Liu, C.J. Lin, J. Lee, X.X. Xu, X.G. Wu, Y. Zheng, C.B. Li, P. Jones, R. A. Bark, Z.H. Wang for their great helps during developmental testing of this GDDAQ. We would also like to thank all the experimental groups using this GDDAQ for their feedback.

References

[1] M. Koskelo, et al., Comparison of analog and digital signal processing systems using pulsers, Nucl. Instrum. Methods Phys. Res. A 422 (1999) 373–378, http://dx.doi.org/10.1016/S0168-9002(98)00986-3.

[2] S. Mitra, et al., Comparison of a digital and an analog signal processing system for neutron inelastic gamma-ray spectrometry, Appl. Radiat. Isot. 61 (2004) 1463–1468, http://dx.doi.org/10.1016/j.apradiso.2004.02.024.

[3] A. Al-Adili, et al., Comparison of digital and analogue data acquisition systems for nuclear spectroscopy, Nucl. Instrum. Methods Phys. Res. A 624 (2010) 684–690, http://dx.doi.org/10.1016/j.nima.2010.09.126.
[4] W.K. Warburton, et al., Current trends in developing digital signal processing electronics for semiconductor detectors, Nucl. Instrum. Methods Phys. Res. A 568 (2006) 350–358, http://dx.doi.org/10.1016/j.nima.2006.07.021.
[5] W. Hennig, et al., Clock and trigger synchronization between several chassis of digital data acquisition modules, Nucl. Instrum. Methods Phys. Res. B 261 (2007) 1000–1004, http://dx.doi.org/10.1016/j.nimb.2007.04.181.
[6] R. Grzywacz, et al., Rare isotope discoveries with digital electronics, Nucl. Instrum. Methods Phys. Res. B 261 (2007) 1103–1106, http://dx.doi.org/10.1016/j.nimb.2007.04.234.
[7] V.K. Utyonkov, et al., Experiments on the synthesis of superheavy nuclei ^{284}Fl and ^{285}Fl in the ^{239,240}Pu + ^{48}Ca reactions, Phys. Rev. C 92 (2015) 034609, http://dx.doi.org/10.1103/PhysRevC.92.034609.
[8] V.K. Utyonkov, et al., Neutron-deficient superheavy nuclei obtained in the ^{240}Pu+^{48}Ca reaction, Phys. Rev. C 97 (2018) 014320, http://dx.doi.org/10.1103/PhysRevC.97.014320.
[9] N.T. Brewer, et al., Search for the heaviest atomic nuclei among the products from reactions of mixed-Cf with a ^{48}Ca beam, Phys. Rev. C 98 (2018) 024317, http://dx.doi.org/10.1103/PhysRevC.98.024317.
[10] S. Pietri, et al., Recent results in fragmentation isomer spectroscopy with rising, Nucl. Instrum. Methods Phys. Res. B 261 (2007) 1079–1083, http://dx.doi.org/10.1016/j.nimb.2007.04.219.
[11] H. Scraggs, et al., TIGRESS highly-segmented high-purity germanium clover detector, Nucl. Instrum. Methods Phys. Res. A 543 (2005) 431–440, http://dx.doi.org/10.1016/j.nima.2004.12.012.
[12] J.-P. Martin, et al., The TIGRESS DAQ/Trigger system, IEEE Trans. Nucl. Sci. 55 (1) (2008) 84–90, http://dx.doi.org/10.1109/TNS.2007.910853.
[13] M. Descovich, et al., In-beam measurement of the position resolution of a highly segmented coaxial germanium detector, Nucl. Instrum. Methods Phys. Res. A 553 (2005) 535–542, http://dx.doi.org/10.1016/j.nima.2005.07.016.
[14] K. Starosta, et al., Digital data acquisition system for experiments with segmented detectors at National Superconducting Cyclotron Laboratory, Nucl. Instrum. Methods Phys. Res. A 610 (2009) 700–709, http://dx.doi.org/10.1016/j.nima.2009.09.016.
[15] P.A. Söderström, et al., Interaction position resolution simulations and in-beam measurements of the AGATA HPGe detectors, Nucl. Instrum. Methods Phys. Res. A 638 (2011) 96–109, http://dx.doi.org/10.1016/j.nima.2011.02.089.
[16] S. Akkoyun, et al., AGATA—Advanced GAmma Tracking Array, Nucl. Instrum. Methods Phys. Res. A 668 (2012) 26–58, http://dx.doi.org/10.1016/j.nima.2011.11.081.
[17] S. Paulauskas, et al., A digital data acquisition framework for the Versatile Array of Neutron Detectors at Low Energy (VANDLE), Nucl. Instrum. Methods Phys. Res. A 737 (2014) 22–28, http://dx.doi.org/10.1016/j.nima.2013.11.028.
[18] S. Lipschutz, et al., Digital data acquisition for the Low Energy Neutron Detector Array (LENDA), Nucl. Instrum. Methods Phys. Res. A 815 (2016) 1–6, http://dx.doi.org/10.1016/j.nima.2016.01.050.
[19] J. Valiente-Dobón, et al., NEDA—NEutron Detector Array, Nucl. Instrum. Methods Phys. Res. A 927 (2019) 81–86, http://dx.doi.org/10.1016/j.nima.2019.02.021.
[20] L. Bardelli, et al., Progresses in the pulse shape identification with silicon detectors within the FAZIA collaboration, Nucl. Instrum. Methods Phys. Res. A 654 (2011) 272–278, http://dx.doi.org/10.1016/j.nima.2011.06.063.
[21] M. Pfützner, et al., Radioactive decays at limits of nuclear stability, Rev. Modern Phys. 84 (2012) 567–619, http://dx.doi.org/10.1103/RevModPhys.84.567.
[22] N.L. Neindre, et al., Comparison of charged particle identification using pulse shape discrimination and ΔE-E methods between front and rear side injection in silicon detectors, Nucl. Instrum. Methods Phys. Res. A 701 (2013) 145–152, http://dx.doi.org/10.1016/j.nima.2012.11.005.
[23] R. Grzywacz, Applications of digital pulse processing in nuclear spectroscopy, Nucl. Instrum. Methods Phys. Res. B 204 (2003) 649–659, http://dx.doi.org/10.1016/S0168-583X(02)02146-8.
[24] C. Prokop, et al., Digital data acquisition system implementation at the National Superconducting Cyclotron Laboratory, Nucl. Instrum. Methods Phys. Res. A 741 (2014) 163–168, http://dx.doi.org/10.1016/j.nima.2013.12.044.
[25] E.C. Pollacco, The transition from silicon to gas detection media in nuclear physics, Nucl. Instrum. Methods Phys. Res. B 376 (2012) 316–320, http://dx.doi.org/10.1016/j.nimb.2016.02.010.
[26] https://www.xia.com/.
[27] https://www.ni.com/en-us.html.
[28] https://www.xia.com/flexible-and-customizable-real-time-solution-interfacing-pixie-16-electronics-to-external-systems.html.
[29] https://root.cern.ch/.
[30] X. LLC, Pixie-16 User Manual, Version 3.04 ed., 2019.
[31] S. Das, et al., A Compton suppressed detector multiplicity trigger based digital DAQ for gamma-ray spectroscopy, Nucl. Instrum. Methods Phys. Res. A 893 (2018) 138–145, http://dx.doi.org/10.1016/j.nima.2018.03.035.
[32] http://zedboard.org/product/microzed.
[33] http://xillybus.com/xillybus-lite.
[34] W. Hennig, et al., Network time synchronization of the readout electronics for a new radioactive gas detection system, IEEE Trans. Nucl. Sci. 66 (2019) 1182–1189, http://dx.doi.org/10.1109/TNS.2018.2885488.
[35] http://docs.nscl.msu.edu/daq/newsite/ddas-1.1/index.html.
[36] A. Fallu-Labruyere, et al., Time resolution studies using digital constant fraction discrimination, Nucl. Instrum. Methods Phys. Res. A 579 (2007) 247–251, http://dx.doi.org/10.1016/j.nima.2007.04.048.